FRAGMENTATION OF RELATIVISTIC ^{56}FE NUCLEI IN EMULSION

G.M. CHERNOV, K.G. GULAMOV, U.G. GULYAMOV, V.SH. NAVOTNY,
N.V. PETROV AND L.N. SVECHNIKOVA.
INSTITUTE OF NUCLEAR PHYSICS, UZBEK ACADEMY OF SCIENCES,
ULUGBEK, TASHKENT 702132, U.S.S.R.

B. JAKOBSSON, A. OSKARSSON AND I. OTTERLUND,
UNIVERSITY OF LUND,
SÖLVEGATAN 14, S-223 62 LUND, SWEDEN.

—— COSMIC AND SUBATOMIC PHYSICS ——

UNIVERSITY OF LUND

SÖLVEGATAN 14

S-223 62 LUND, SWEDEN

Fragmentation of relativistic ^{56}Fe nuclei in emulsion

G.M. Chernov, K.G. Gulamov, U.G. Gulyamov, V.Sh. Navotny,
N.V. Petrov and L.N. Svechnikova.
Institute of Nuclear Physics, Uzbek Academy of Sciences,
Ulugbek, Tashkent 702132, U.S.S.R.

B. Jakobsson, A. Oskarsson and I. Otterlund,
University of Lund,
Sölvegatan 14, S-223 62 Lund, Sweden.

Fragmentation of Relativistic ^{56}Fe Nuclei in Emulsion.

G.M. Chernov, K.G. Gulamov[*], U. G. Gulyamov, V.Sh. Navotny[*],
N.V. Petrov and L.N. Svechnikova[*].
Institute of Nuclear Physics, Uzbek Academy of Sciences,
Ulugbek, Tashkent 702132, U.S.S.R.

B. Jakobsson, A. Oskarsson and I. Otterlund,
University of Lund,
Sölvegatan 14, S-223 62 LUND, Sweden.

Abstract
Experimental data on general characteristics of projectile
fragments in inelastic interactions of relativistic ^{56}Fe nuc-
lei in emulsion (multiplicities, transverse momentum distri-
butions, azimuthal correlations) are presented and discussed.

A strong dependence on the mass number of the projectile nuc-
leus is observed for the transverse momenta of the emitted
projectile fragments. These fragments exhibit an azimuthal
asymmetry caused by the transverse motion of the fragmenting
residue, but it is shown that this motion can be responsible
only for a part of the increase in the average transverse
momentum of the fragments with increasing mass of the projec-
tile.

---

[*] Permanent address: S.V. Starodubtsev Physical Technical
Institute, Tashkent 700084, U.S.S.R.

1.   Introduction.

Fragmentation of relativistic projectile nuclei is in general a relatively well isolated process in the complex scheme of high energy reactions between multibaryon systems. The experimental knowledge of this process is essential for studies of how the heavy cosmic ray spectrum is changed during the transport through universe.

The first experimental information about fragmentation of nuclei was in fact obtained in experiments with cosmic ray particles -- see, e.g. [1,2]. Acceleration of heavy ions up to relativistic energies at Berkeley and Dubna gave an opportunity of more detailed studies of this phenomenon and a number of papers, both experimental and theoretical, have been published during the last decade on the fragmentation of light nuclei ($A_p \lesssim 16$) [3 and references therein].

Fragmentation of accelerated iron nuclei have been considered more recently in refs. [3,4]. The experimental data on the yield of projectile fragments with charges $Z \geq 13$ were presented in [3]. In ref. [4] it was experimentally observed that in inelastic collisions of ^{56}Fe nuclei in emulsion the angular distribution of "spectator" alpha-particles became considerably wider than in analogous interactions of ^{16}O nuclei.

In the present paper we report on experimental data for fragmentation of ^{56}Fe nuclei in emulsion at an incident momentum of 2.5 GeV/c per nucleon. We discuss the yield of projectile fragments with charges $Z = 1-8$ and $Z \geq 9$ from collisions with light and heavy emulsion nuclei. The factorization of fragmentation cross-sections, transverse momentum distributions and correlations between projectile fragments in the azimuthal plane are discussed after comparison with data from ^{12}C and ^{14}N induced reactions.

2.   Experimental Material.

The experiment has been performed in a stack of Ilford G5

nuclear emulsions exposed at the LBL (Berkeley) to a beam of
^{56}Fe ions with kinetic energy 1.9 GeV per nucleon. The ioni-
zation losses of the primary nuclei in emulsion before the
interactions reduce the average incident momentum for Fe-Em
collisions to (2.5 ± 0.1) GeV/c per nucleon ($<E_{kin}>$ =
= (1.7 ± 0.1) GeV per nucleon).

On the total length of 109.8 m of scanned primary tracks we
have registrated 1308 interactions which corresponds to the
mean free path of ^{56}Fe nuclei in emulsion equal to (8.4±0.2) cm.
Events without charged secondary particles, production of ener-
getic δ-electrons and e^+e^- pairs were not registrated. Events
close to the surface and glass were removed. The remaining
980 Fe-Em interactions were used for further analysis. Char-
ged secondaries in these events were classified into the fol-
lowing types: "black" or b-particles with the range in emulsi-
$\ell \leq 3$ mm ($E_{proton} \leq 26$ MeV), "grey" or g-particles with $\ell \geq 3$ m.
and velocity $\beta = v/c < 0.7$ (26 < E_{proton} < 375 MeV), shower
or s-particles - singly charged particles with $\beta > 0.7$ and
"noninteracting" fragments of the projectile nucleus (f-partic-
les) with charge $Z \geq 2$. For b- and g-particles altogether
one uses the term "heavy track producing particles". The po-
lar, Θ, and azimuthal, Φ, emission angles were measured for
all charged secondary particles. The errors in the angles
have been estimated from repeated measurements on tracks from
real events and on tracks from pseudo-events. In the latter
case we initiated a one-prong-event by chosing an arbitrary
point on a straight track as the centre of the event. In this
pseudo-event there is one prong from the "incident" particle
and one forward prong from the "emitted" particle. We measu-
red the angle of this forward prong on tracks with different Z.
The uncertainties in angles on relativistic tracks with Θ < 5°
is ΔΘ ≈ ± 0.1°.

In the present paper we are discussing characteristics of non-
interacting (spectator) fragments from the projectile iron
nuclei (hereafter called fragments). They include all f-partic-
les and a part of the s-particles.

Selection of f-particles in nuclear emulsions can easily
be performed since these tracks are characterized by high

ionization which, in contrast to b- and g-particles, does
not change over large distances (several cm). Furthermore
they do not reveal noticeable multiple scatterings. The
charges of f-particles have been determined by measurements
of the number of gaps and δ-electrons on a track length of
more than 1 cm. This method allows the identification of the
charge in the range $2 \leq Z \leq 8$ with an accuracy which is better
than ± 1. For $Z \geq 9$ the error in the charge measurements is
of the order of one unity or larger and therefore fragments
with $Z \geq 9$ will be considered subsequently as one subgroup.

It is more difficult to identify singly charged projectile
fragments. For this purpose we use a statistical method based
on the comparison of angular distributions of s-particles
produced in nucleus-nucleus and proton-nucleus collisions at
the same energy per nucleon. We assume that the angular
distribution of singly charged projectile fragments in the
laboratory frame can be written as

$$\frac{dN}{d\cos\theta} \sim A_F^2 p_O^2 \cos\theta \exp\left[-A_F^2 p_O^2(1-\cos^2\theta)/2\sigma^2\right] \tag{1}$$

where A_F is the mass number of a fragment and p_O is the in-
cident momentum per nucleon. Formula (1) corresponds to a
transverse momentum distribution of the type

$$\frac{dN}{dp_\perp} = \frac{p_\perp}{\sigma^2} \exp\left(-p_\perp^2/2\sigma^2\right) \tag{2}$$

The experimental data on pA collisions show (5) that the an-
gular distribution of "produced" s-particles at small emis-
sion angles θ can be written as:

$$\frac{dN}{d\cos\theta} = \text{const.} \tag{3}$$

We have fitted the angular distribution of s-particles in
Fe-Em interactions to a sum of the distributions (1) and (3)
- see Figure 1. This procedure allows one to determine the
angle θ_O which is meant to separate s-particles of fragmen-
tation type $(\theta < \theta_O)$ and s-particles produced in more vio-

lent processes $(\theta > \theta_o)$. The value of θ_o is chosen in such a way that the number of fragments with $\theta > \theta_o$ is equal to the number of "produced" s-particles having $\theta < \theta_o$. We have found that the contribution of "produced" relativistic particles in the region $\theta < \theta_o$ is approximately 12 % of all s-particles here. The use of a "limiting" angle θ_o is quite reasonable when estimating average multiplicities of singly charged fragments in different ensembles of Fe-Em interactions. We found that the described procedure of fragment separation is weakly (if at all) dependent on the mass of the target nucleus. Of course when estimating $p_\perp$-distributions for singly charged fragments the tails of the θ-distributions should be taken into account. This has been done under additional assumptions about the contributions of protons, deuterons and tritons, based on the well-known experimental data on fragmentation of nuclei obtained in spectrometer experiments [6].

We have separated the Fe-Em interactions into ensembles of collisions with hydrogen (Fe-H, $A_T=1$), light (Fe-CNO,$<A_T>=14$) and heavy (Fe-AgBr,$<A_T>=94$) emulsion nuclei. Fe-H collisions were selected using constraints on n_h, the multiplicity of heavily ionizing particles, kinematics of the event and features of p-Em collisions in the antilaboratory frame, based on the experimental data on proton-nucleus interactions. The detailed description of this procedure will be published elsewhere. From 179 events satisfying the necessary criteria of Fe-H interactions in emulsion, we have excluded 45 two-prong stars, one prong being the projectile with unchanged ionization and the second one being the black track of a recoil proton, satisfying the kinematics of elastic Fe-proton scattering. The remaining events with $n_h \leq 8$ (events with $n_h > 8$ are Fe-AgBr collisions) ere divided into Fe-CNO and Fe-AgBr interactions following the method described for pA interactions in ref. [7]. Below we analyse 134 Fe-H, 319 Fe-CNO and 482 Fe-AgBr inelastic interactions.

It should be noted that when analysing the data we consider

in all cases the uncertainties in identification of the target mass and in the separation of singly charged fragments. When these problems are not specially discussed, they are small and cannot change any conclusion.

3. Multiplicity of Fragments.

In Table 1 we present data on the average multiplicity of fragments with different charge, Z, in interactions of iron nuclei in emulsion. Only statistical errors are quoted. The possible systematic errors due to the above-mentioned uncertainties in the identification are estimated to be of the same order (for Z=1) or smaller (for $Z \geq 2$ fragments) than the statistical ones. Measurements of Fe fragmentation $(13 \leq Z_F \leq 25)$ have been performed by Westfall et al. [3]. A parametrisation of the existing data in the spirit of limiting fragmentation results in the multiplicities $\langle n_{9-25} \rangle =$ = 0.9 and $\langle n_{9-25} \rangle = 0.7$ for fragments in the charge group $9 \leq Z_F \leq 25$ for ^{56}Fe-H and ^{56}Fe-CNO reactions respectively. These multiplicities are similar to those in Table 1 while the value $\langle n_{9-25} \rangle = 0.4$ estimated for Fe-AgBr reactions is larger than that obtained in this experiment.

In Fig. 2 we show the multiplicity distributions of fragments with Z = 1 and 2. Multiplicities n > 1 for heavier fragments are very rare. For Z=3 and 4 we observe the percentage $W(n_{Z=3,4} > 1) = 3.2$ %. For Z = 5-8 we found $W(n_{Z=5-8} > 1) =$ = 1.3 % while no events are registered with $n_{Z>9} > 1$. The average multiplicity of fragments with Z < 9 in Fe-H collisions can be compared with the multiplicity of evaporation or black particles in p-Em collisions at a primary momentum of 3.1 GeV/c [9]. The multiplicities to be compared are $\langle n_{Z<9} \rangle$ (Fe-H) = 3.60 ± 0.23 and $\langle n_b \rangle$ (pEm) = 3.83 ± 0.11. Taking into account that at these energies, $\langle n_b \rangle \sim A^\alpha$ where α is 0.56 ± 0.03 [9] and A is the target mass in p-A collisions, one estimates $\langle n_b \rangle$ (p-Fe) $\approx$ 3.5. Thus, we conclude that the average multiplicity of fragments in events classified as Fe-H collisions is in good agreement with that of the target multiplicity in p-Fe interactions.

Inclusive experiments in which forward emitted ($\theta < 0\overset{\circ}{.}7$)
fragments of light nuclei were detected with a spectrometer
[6,10,11] observed that fragmentation cross-sections could
be factorized; $\sigma_{PT}^{F} = \gamma_{P}^{F}\gamma_{T}$, where designations P,T,F belong
to the projectile, target and fragment, respectively. In
other words, the charge composition does not depend on the
target nucleus. The target factor γ_{T} depends weakly on A_{T}

$$\gamma_{T} \sim A_{T}^{1/4} \tag{4}$$

In 4π experiments, where the total fragmentation cross-sec-
tions are measured, the exact factorization is found to be
invalid. In Table 2 we present some examples illustrating
the dependence of multiplicity ratios on the mass number of
the target nucleus. Table 3 compares the values of the mul-
tiplicity ratio $\langle n_{z}\rangle_{AgBr}/\langle n_{z}\rangle_{CNO}$ for fragmentation of iron
and nitrogen nuclei. Note that the data on fragmentation of
^{14}N nuclei [12] were obtained at $p_{0} = 2.9$ GeV/c per nucleon.
The experimental conditions were identical to those of the
present experiment.

The following can be concluded:

1. In contrast to fragmentation of ^{14}N nuclei, where multi-
plicities of fragments with any Z decrease with increasing A_{T},
multiplicities of light ($Z \leq 8$) fragments from ^{56}Fe nuclei
increase with the target mass number (Table 1). Only the mul-
tiplicity of heavy residual fragments of iron nuclei decrea-
ses with increasing A_{T}. Note also that the increase of multi-
plicities of light fragments (c.f. Table 1) does not satisfy
equation (4) which gives ratios independent of the target mass.

2. The composition of fragments from nitrogen nuclei depends
considerably on A_{T} for any Z-value (c.f. Table 3), thus
showing that the factorization is broken in interactions of
^{14}N nuclei in emulsion (see also [12]). The composition of
fragments is the same within experimental uncertainties for all
ensembles of Fe-events (Fe-H, Fe-CNO, Fe-AgBr) again with
the exception for the case of heavy fragments.

Thus, the factorization of fragmentation cross sections observed at zero angle has probably a restricted region of applicability. It is broken for the integrated cross sections and the deviation from simple fragmentation increases with the mass of the incident nucleus. We show below (section 5) that the emission of projectile fragments in interactions induced by relativistic ^{56}Fe-nuclei are quite different from the fragmentation of light nuclei (like N) and can only partially be explained by Fermi motion.

4. Transverse Momentum Distributions.

Much information about the dynamics of the fragmentation process could be obtained from analysis of momentum distributions of fragments. An important result found in previous experiments is that the momentum components of a fragment have approximately a universal (gaussian) shape in the rest frame of the fragmenting nucleus [6]. The dispersion of this distribution has a parabolic dependence on the mass of the fragment [6]. These regularities follow naturally from the statistical approach to the fragmentation process with minimal correlations between momenta of intranuclear nucleons.

However, in 4π experiments (mainly emulsion experiments – see, e.g. [12,14,15]) it is observed that transverse momentum distributions of fragments can have large $p_\perp$ tails, indicating the existence of a non-statistical contribution. The contribution of these high $p_\perp$ tails is comparatively small for the fragmentation of light (^{16}O) projectiles, except in interactions where only one light (Z = 2-3) fragment is emitted [14].

In the present section, we compare fragmentation of ^{56}Fe nuclei with ^{14}N and ^{12}C nuclei in emulsion at 2.9 and 4.5 GeV/c per nucleon, respectively [12,15]. Note that all the experimental data considered were obtained and processed under the same experimental conditions, except for the beam momentum.

In all cases the transverse momentum of a fragment was cal-
culated on the basis of its emission angle

$$P_\perp = A_F P_O \sin \theta .$$ (5)

It has been shown in [12,15] that for Z = 1 the values of
$P_\perp$ calculated from eq. (5) agree well with those obtained
on the basis of momentum measurements. For Z $\geq$ 2 we make
the assumption that the mass number of the fragment A_F is 2Z.
Due to the general excess of neutron-rich isotopes for Z $\geq$ 3
(see, e.g. review in [16]) eq. (5) gives a lower limit for the
average transverse momentum.

In Table 4 we present the average values of transverse momen-
ta of fragments in ^{14}N-Em, ^{12}C-Em and ^{56}Fe-Em interactions.
The most obvious feature of these data is the considerable
rise of the average transverse momentum for all Z values when
comparing ^{12}C- and ^{14}N- with ^{56}Fe-reactions. Assuming that in
the range $12 \leq A_p \leq 56$, $<p_\perp>$ can be parametrized as $<p_\perp> \sim A_p^\alpha$,
one obtains $\alpha = 0.25 \pm 0.03$ for fragments with Z=2 and
$0.3 \lesssim \alpha \lesssim 0.5$ for heavier fragments. For singly charged frag-
ments we can unfortunately determine only the lower limits of
$<p_\perp>$ due to the use of an a priori postulated spectrum (1).
If one uses this spectrum (1) also for identified fragments
with Z $\geq$ 2, i.e. when neglecting the "tails" of $p_\perp$-distribu-
tions (see below), one obtaines $<p_\perp>$ values which are signi-
ficantly lower than those listed in Table 4.

Note also that the neutron excess of the fragments (i.e. when
$A_F > 2Z_F$) can only strengthen the observed rise of $<p_\perp>$ in
Fe-Em interactions in comparison with collisions of light pro-
jectiles.

The effect discussed here was observed first in cosmic ray
reactions more than 25 years ago [1] - mostly for alpha-par-
ticles. Recently it has also been observed and discussed in

an accelerator experiment, when comparing the angular dist-
ributions of α-particles in ^{56}Fe-Em and ^{16}O-Em collisions [4].

In Table 5 we show the values of $\langle p_\perp \rangle$ in interactions of ^{56}Fe
ions with different target nuclei. The data exhibit a rise
of $\langle p_\perp \rangle$ with the mass of the target. Using again the power
approximation $\langle p_\perp \rangle \sim A_T^\beta$ one obtains $\beta \simeq 0.05$, i.e. a much
weaker dependence on A_T than on A_p.

Transverse momentum distributions of fragments with different
charges are shown in Figs. 3-5. In Fig. 3 we compare
$p_\perp$-distributions of fragments in interactions of different pro-
jectile nuclei in emulsion. The corresponding distributions
in interactions of ^{56}Fe ions with different components of emul-
sion are shown in Fig. 4. Fig. 5 compares the $p_\perp$-distribu-
tions of fragments with $Z = 2$ and $3 \leq Z \leq 4$ with the universal
gaussian distribution (eq. (2) with $\sigma = (\langle p_\perp^2 \rangle / 2)^{\frac{1}{2}}$) which
corresponds to the statistical mechanism of fragmentation.
Distributions for fragments with $Z=1$ are shown in Figs. 3
and 4 only for the completeness; one should remember that
they are based on formula (2) thus a priori excluding high
values of $p_\perp$.

The following can be concluded from these data:

1. $p_\perp$-distributions for fragments with $Z \geq 2$ in Fe-Em in-
teractions are shifted considerably towards large $p_\perp$ values
in comparison to corresponding distributions for light projec-
tile nuclei.

2. The $p_\perp$-distributions depend weakly on A_T (Fig. 4 and
Table 5). It should be noticed that even in Fe-H collisions
the $p_\perp$-distributions differ from those in collisions of light
projectile nuclei (see also Tables 4 and 5). Thus the fea-
tures of fragmentation are more dependent on the mass number
of the fragmenting nucleus than the partner nucleus.

3. $p_{\perp}$-distributions for fragments of all charges cannot be well described by a simple gaussian function (c.f. Fig. 5). The well-known parabolic dependence of the widths of the momentum distributions on the charge of fragments remain approximately valid also in Fe-Em interactions. In Fig. 6 we show the dependence of $\langle p_{\perp} \rangle$ (note that $\langle p_{\perp} \rangle = \sqrt{\frac{\pi}{2}}\,\sigma$) on Z for $2 \leq Z \leq 8$ in Fe-Em collisions. It is seen that this dependence can be described by a function

$$\sigma^2 = \sigma_o^2 2Z(A_p - 2Z)/(A_p - 1) \tag{6}$$

but only if σ_o is large (σ_o = 140 MeV/c). If one formally uses the known relations of the Fermi gas model [13], σ_o = $\langle p^2 \rangle / 3$ and $\langle p^2 \rangle = 3p_F^2/5$ ($\langle p^2 \rangle$ is the mean square momentum of uncorrelated nucleons in a nucleus and p_F the Fermi momentum) the values of p_F obtained from the experimental data ($p_F \approx 0.32$ GeV/c) come out to be too high.

5.   Azimuthal correlations.

One reason for the large average transverse momentum of fragments could be that a momentum transfer to the residual nucleus is taking place prior to the fragmentation. A transverse motion of the fragmenting residue should lead to an azimuthal asymmetry of the fragmentation products.

In order to study azimuthal correlations between fragments we studied the following quantities:

a)   the coefficient of azimuthal asymmetry

$$A = \left(\int_{\pi/2}^{\pi} f(\epsilon)\,d\epsilon - \int_{0}^{\pi/2} f(\epsilon)\,d\epsilon\right)\bigg/\int_{0}^{\pi} f(\epsilon)\,d\epsilon \tag{7}$$

of the inclusive distribution ($f(\epsilon) = \frac{1}{\sigma}\frac{d\sigma}{d\epsilon}$). The angle we study is $\epsilon \equiv \epsilon_{ij} = \arccos\,[(\vec{p}_{\perp i}\cdot\vec{p}_{\perp j})/|\vec{p}_{\perp i}\cdot\vec{p}_{\perp i}|]$ i.e. the angle between the transverse momenta of the i-th and the j-th fragment from an event ($0 \leq \epsilon \leq \pi$);

b)   the average value of the coefficient of azimuthal asymmetry in individual events

$$\langle\alpha\rangle = \sum_{k=1}^{N} \alpha_k/N, \quad \alpha_k = \sum_{i\neq j}^{n_k} \cos\epsilon_{ij}/\sqrt{n_k(n_k-1)} \qquad (8)$$

where $k = 1,2 \ldots, N$; N being the number of events in the ensemble with a multiplicity $n_k \geq 2$ of fragments of considered type.

Let us remember some properties of the equations (7) and (8), useful for the proceeding analysis.

1.   Under the assumptions of uncorrelated emission of fragments and isotropy of fragment angular distributions the ϵ_{ij}-distribution is uniform in the interval $[0,\pi]$ and the average values of A and $\langle\alpha\rangle$ are equal to zero.

2.   The fragments i and j can belong to a group of particles, which are produced according to the phase-space integral with a transverse part of the form:

$$\frac{d\sigma^{(n)}}{dp_{\perp 1}\ldots dp_{\perp n}} = \prod_{i=1}^{n} \Phi(p_{\perp i})\delta^{(n)}\left(\sum_{i=1}^{n}p_{\perp i}\right) \qquad (9)$$

(n is the total number of fragments, $\Phi(p_{\perp i})$ is the "cut-off" function, which takes into account that the transverse momenta of fragments are restricted). The decay of some "fireball" is an example of such a production mechanism. The expectation values of A and $\langle\alpha\rangle$ will then be:

$$M(A) = \langle n_k(n_k-1)/(n-1)\rangle/\langle n_k(n_k-1)\rangle,$$

$$M(\langle\alpha\rangle) = -(\pi/4)\langle[n_k(n_k-1)]^{\frac{1}{2}}/(n-1)\rangle \qquad (10)$$

Here the averaging is performed over events with a multiplicity of charged fragments $n_k \geq 2$. Formulas (10) correspond to the choice of the transverse momentum distribution $\Phi(p_{\perp i})$ in the form of eqn. (2). The model with a matrix element

of type (9) is generally called the cylindrical phase-space
(CPS) model. One can see from eq. (10) that the transverse
momentum conservation leads to the inequalities $A > 0$, $\langle\alpha\rangle < 0$
and the ϵ_{ij}-distribution has a maximum at $\epsilon_{ij} = \pi$ in this
case.

3. If the decaying "fireball" has a transverse momentum
this would lead to a decrease of A and an increase of $\langle\alpha\rangle$
in contrast to the momentum conservation. The ϵ-distribu-
tion reveals in this case a tendency to have a maximum
at $\epsilon = 0$.

Let us now consider the experimental data. In Fig. 7 we
show ϵ_{ij} and α_k-distributions for fragments with $Z \geq 2$ in
Fe-Em interactions. Values of A and $\langle\alpha\rangle$ in different en-
sembles of collisions are listed in Table 6. One can con-
clude from these data, that:

i) The transverse momentum distributions of fragments are
asymmetrical in the azimuthal plane. This fact gives evi-
dence for that the fragmenting nucleus has a transverse mo-
mentum.

ii) The azimuthal asymmetry of fragments increases with the
mass number of the target.

The latter statement follows from the data of Table 6. We
see from Table 6 that A and $\langle\alpha\rangle$ are equal to zero in Fe-H
collisions. This does not mean that projectile fragments
in Fe-H collisions are not correlated in the azimuthal plane.
In fact, under reasonable assumptions about the total multi-
plicity of fragments, (see below), the transverse momentum
conservation alone produces expectation values of A and $\langle\alpha\rangle$
in Fe-H interactions of $A = 0.2$ and $\langle\alpha\rangle = -0.4$.

We have performed Monte Carlo calculations for Fe break-up in the picture of a fragmentation model, based on the following assumptions:

1. The residual nucleus decays according to the cylindrical phase-space model (CPS) into n_1 singly charged, n_2 doubly charge n_3 multiply charged $(Z \geq 3)$ and n_o neutral fragments.

2. The transverse momenta of the fragments are distributed according to eq. (2). $\langle p_\perp \rangle$ values for fragments with $Z = 1,2,$ ≥ 3 are taken from table 4 (values from ^{12}C-Em and ^{14}N-Em are used) and furthermore we assume $\langle p_\perp \rangle_{Z=0} = \langle p_\perp \rangle_{Z=1}$.

3. The fragmenting nucleus has a transverse momentum, $p_\perp^n$, superimposed on the "internal" transverse momenta of fragments. $p_\perp^n$ was considered as an adjustable parameter.

When performing the calculations we use (Table 1) $n_1 = 3$. It is assumed that the number of protons among singly charged fragments multiplied by $(A-Z)/Z$ for ^{56}Fe is equal to the number of neutrons (n_o), $n_3 = 1$ and $n_2 = 2$ or 3 (the average number of α-particles in events with $n_{Z \geq 2} \geq 2$ is equal to 2.5).

The most serious assumption here is the choice of σ (and $\langle p_\perp \rangle$) values which should characterize the internal Fermi motion of the nucleons within the fragmenting nucleus. It is reasonable to use the empirical values from fragmentation of light nuclei rather than to apply some speculative assumptions. It is, however, necessary to remember that the empirical values of $\langle p_\perp \rangle$ and σ in fragmentation of light nuclei are probably larger than the real ones because: a) the possible nonstatistical contribution of high $p_\perp$ tails, and b) in fragmentation of light nuclei there may also exist a transverse motion of the residue which increase $\langle p_\perp \rangle$ just as in the case of ^{56}Fe fragmentation. However, this can only strengthen our conclusions.

The main results of our calculations are presented in Figs. 7-9. The following conclusions can be drawn:

1.   The presence of a transverse momentum $p_\perp^n$ ensures the azimuthal asymmetry of fragments. All the quantitative characteristics of azimuthal asymmetry for fragments with $Z \geq 2$ in Fe-Em interactions - the average values A and $\langle \alpha \rangle$ (Fig. 8), ϵ_{ij} - and α_k-distributions (Fig. 7) - can be described reasonably well by the model with a transverse momentum of the fragmenting residual nucleus of $|p_\perp^n| = (0.15 \pm 0.01)$ GeV/c. It is necessary to point out that if we decrease the "input" values of $\langle p_\perp \rangle$ (and σ) for projectile fragments, then the magnitude of $|p_\perp^n|$ would increase.

2.   In order to describe the observed large average transverse momenta of fragments from ^{56}Fe in comparison to the "input" values of $\langle p_\perp \rangle$, it is necessary to have considerably higher values of $|p_\perp^n|$. In Fig. 9 we see that for fragments with $Z=2$ (α-particles) the $|p_\perp^n|$ value needed is (0.32 ± 0.02) GeV/c. It is important to notice that if one decreases the "input" - values of $\langle p_\perp \rangle$, the corresponding value of $|p_\perp^n|$ describing the experimental data on transverse momenta of fragments would increase. In other words the values of the transverse momentum of the fragmenting residual nucleus, describing the observed azimuthal asymmetry, can explain only a small part ($\sim$ 20-30%, see Fig. 9) of the increase of $\langle p_\perp \rangle$ with increasing mass of the projectile nucleus.

Finally it should be pointed out that our calculated $\langle p_\perp \rangle$ - $|p_\perp^n|$ relation depends rather weakly on the assumptions of the multiplicities of fragments of different types in Fe-Em interactions.

6.   Discussion and Conclusions.

Let us briefly summarize the main experimental observations of the present investigation and formulate the conclusions which can be drawn.

1.   Transverse momentum distributions of fragments have
tails of large $p_\perp$, which cannot be described by a simple
statistical model of fragmentation with no correlations bet-
ween intranuclear nucleons.

2.   The transverse momenta of projectile fragments have a
strong dependence on the mass number of the projectile nuc-
leus and a weaker dependence on the mass of the target.   The
mean transverse momentum of the fragments increases with in-
creasing A_p and A_T.

3.   The emission of fragments is asymmetrical in the azimut-
hal plane, which could mean that the fragmenting residual
nucleus gets a transverse momentum during the collision
process.

4.   A transverse momentum of the fragmenting nucleus can,
however, be responsible only for a minor part of the A_p-de-
pendence observed for the mean transverse momentum of the
fragments.   The main part must therefore be attributed to
the dynamics of nucleus-nucleus interactions and/or struc-
ture effects.

Qualitatively, the observed effects may be due to multiple
rescattering, hard processes, short-range intranuclear cor-
relations, coulomb repulsion between clusters, collective
nuclear fluid effects and so on.

On the other hand, the data allow to draw some model inde-
pendent conclusions.   Our data indicate for example that the
partner-nucleus is not a simple spectator of the fragmenta-
tion process.

It is necessary to remember that in the present paper we have
not discussed the longitudinal momentum distributions of pro-
jectile fragments which are less sensitive to the dynamics
of nucleus-nucleus interactions (see e.g. [18]).   Another com-
ment concerns the projectile fragmentation as a probe of the
Fermi momentum distribution.   The results of the present in-
vestigation show, that the real situation is complicated and

it seems that information about the internal motion cannot
be obtained (in a model-independent way) from the data on
transverse momentum distribution of fragments.

References

1. C.F. Powell, P.H. Fowler and D.H. Perkins, Study of elementary particles by the photographic method (Pergamon, London, 1959).

2. V.S. Barashenkov and V.D. Toneev, Interactions of high-energy particles and atomic nuclei with nuclei (Atomizdat. Moscow, 1972).

3. G.D. Westfall et al., Phys. Rev. C19 (1979) 1309.

4. K.B. Bhalla et al., Nucl. Physics A367 (1981) 446.

5. E.S. Basova et al., Yadernaya Fizika 34 (1981) 1524.

6. D.E. Greiner et al., Phys. Rev. Lett. 35 (1975) 152.

7. Alma-Ata - Leningrad - Moscow - Tashkent collaboration, Yadernaya Fizika 22 (1975) 736; K.G. Gulamov et al., in Multiparticle processes at high energies (Fan, Tashkent, 1976) 78.

8. T. Saito, J. Phys. Soc. Japan 30 (1971) 1243.

9. E.S. Basova et al., Doklady of Uzbek Academy of Sciences 8 (1980) 28; 9 (1981) 31.

10. H.H. Heckman et al., Phys. Rev. Lett. 28 (1972) 926.

11. P.J. Lindstrom et al., Lawrence Berkeley Laboratory report LBL-3650, 1975.

12. A.I. Bondarenko et al., Izvestiya of Uzbek Academy of Sciences, Phys. and math. Sciences, 2 (1979) 73.

13. A.S. Goldhaber; Phys. Lett. B53 (1974) 306.

14. B. Jakobsson et al., Lett. Nuovo Cimento 15 (1976) 444.

15. Bucharest – Warzaw – Dubna – Kosiĉe – Leningrad –
     Moscow – Tashkent collaboration, Yadernaya Fizika 32
     (1980) 1387.

16. B. Jakobsson, C.R.N. de Strasbourg report
     CRN/PN 77-3, 1977.

17. S.A. Azimov and G.M. Chernov, Statistical methods in
     high-energy physics (Fan, Tashkent, 1970);
     S.A. Azimov et al., in Multiparticle processes at high
     energies (Fan, Tashkent, 1976) 120.

18. T. Fujita and J. Hüfner, Nucl. Phys. A343 (1980) 493.

Figure captions.

Figure 1. Angular distributions of s-particles in Fe-Em in-
teractions. The solid curve represents the fit
to the data ($x^2/D.O.F. = 1.2$) by the sum of distri-
butions (1) and (2) (dashed lines).

Figure 2. Multiplicity distributions of singly (a,c) and
doubly (d,b) charged fragments in:
a,b: Fe-Em interactions.
c,d: Fe-H-interactions (dotted histogram).
c,d: Fe-AgBr interactions (solid histogram).

Figure 3. Transverse momentum distributions of fragments
with $Z = 1$ (a), 2 (b), 3-4 (c) and 5-6 (d) in
^{12}C-Em, ^{14}N-Em and ^{56}Fe-Em collisions (the dotted,
dashed and solid histogram, respectively).

Figure 4. The same as in Fig. 3, but for Fe-H (dotted), Fe-CNO
(dashed) and Fe-AgBr (solid histogram) collisions.

Figure 5. A comparison between experimental $p_\perp$-distributions
for fragments with $Z=2$ (a) and 3-4 (b) and a gaus-
sian distribution eq. (6).

Figure 6. $\langle p_\perp \rangle$ as a function of Z in Fe-Em collisions. The
curve exhibits the parabolic dependence described
by eq. (7).

Figure 7. Distributions of quantities ϵ_{ij} (a) and α_k (b) in
Fe-Em collisions for fragments with $Z \leq 2$. The
solid histogram exhibits experimental data. The
curve 1 and dotted histogram represent the cylind-
rical phase-space model (CPSM) calculations (see
the text) with $|p_\perp^n|=0$ while the curve 2 and the
dashed histogram correspond to the CPSM with
$|p_\perp^n| = 0.15$ GeV/c.

Figure 8. Predictions of the CPSM for the dependence of A (a)
and $\langle \sigma \rangle$ (b) on $|p_\perp^n|$ for fragmemts with $Z \geq 2$.

Figure 9. Dependence of $\langle p_\perp \rangle$ for fragments with $Z<2$ on $|p_\perp^n|$ calculated from the CPSM described in the text.

Table 1. Multiplicities of projectile fragments in interactions of relativistic ^{56}Fe nuclei in emulsion.

Charge of fragments Z	$\langle n_Z \rangle$			
	Fe-H	Fe-CNO	Fe-AgBr	Fe-Em
1	2.35 ± 0.17	3.00 ± 0.13	3.24 ± 0.09	3.03 ± 0.06
2	1.17 ± 0.11	1.61 ± 0.10	1.75 ± 0.07	1.62 ± 0.05
3	0.06 ± 0.03	0.11 ± 0.02	0.17 ± 0.02	0.13 ± 0.01
4		0.08 ± 0.02	0.06 ± 0.01	0.06 ± 0.01
5	0.02 ± 0.01	0.05 ± 0.01	0.05 ± 0.01	0.04 ± 0.01
6		0.04 ± 0.01	0.06 ± 0.01	0.04 ± 0.01
7		0.04 ± 0.01	0.06 ± 0.01	0.05 ± 0.01
8		0.04 ± 0.01	0.04 ± 0.01	0.04 ± 0.01
9 - 26	0.98 ± 0.01	0.64 ± 0.03	0.26 ± 0.02	0.49 ± 0.02

Table 2. Charge composition of projectile fragments in inter-
actions of ^{14}N and ^{56}Fe ions with nuclei of emulsion.

ratio of multiplicities	Projectile nucleus	target-nucleus		
		H	CNO	AgBr
$\dfrac{\langle n_{Z=2}\rangle}{\langle n_{Z=1}\rangle}$	^{14}N	0.90 ± 0.07	0.78 ± 0.04	0.61 ± 0.04
$\dfrac{\langle n_{Z=2}\rangle}{\langle n_{Z=1}\rangle}$	^{56}Fe	0.50 ± 0.06	0.54 ± 0.04	0.54 ± 0.03
$\dfrac{\langle n_{Z\geq 3}\rangle}{\langle n_{Z=2}\rangle}$	^{14}N	0.31 ± 0.04	0.29 ± 0.03	0.20 ± 0.04
$\dfrac{\langle n_{Z\geq 9}\rangle}{\langle n_{Z=2}\rangle}$	^{56}Fe	0.84 ± 0.01	0.40 ± 0.02	0.15 ± 0.01

Table 3. The ratio of the average multiplicities of
projectile fragments produced on heavy and
light nuclei of emulsion.

Charge of fragments Z	$\langle n_Z\rangle_{AgBr} / \langle n_Z\rangle_{CNO}$	
	^{56}Fe	^{14}N
1	1.1 ± 0.05	0.73 ± 0.04
2	1.1 ± 0.08	0.57 ± 0.04
3-4	1.2 ± 0.1	0.39 ± 0.08
5-8	1.2 ± 0.1	
≥ 9	0.41 ± 0.03	

Table 4. Average transverse momenta of projectile fragments
in interactions of relativistic nuclei in emulsion

Charge of fragments Z	$\langle p_\perp \rangle$ in GeV/c		
	^{12}C-Em [15]	^{14}N-Em [12]	^{56}Fe-Em
1	0.13 ± 0.01	0.12 ± 0.01	0.14 ± 0.01
2	0.24 ± 0.01	0.24 ± 0.01	0.37 ± 0.01
3	0.29 ± 0.02	0.24 ± 0.02	0.42 ± 0.03
4	0.23 ± 0.02	0.29 ± 0.02	0.51 ± 0.04
5	0.27 ± 0.04	0.25 ± 0.02	0.51 ± 0.06
6	0.27 ± 0.05	0.33 ± 0.03	0.53 ± 0.06
7	-	0.33 ± 0.09	0.60 ± 0.06
8	-	-	0.53 ± 0.05
≥ 9	-	-	0.52*)

*) A crude estimate based on the angular distribution of
fragments with Z ≥ 9 and the data of ref. [3] on Z-dist-
ributions of fragments with Z ≥ 13.

Table 5.   Average transverse momenta of fragments in different ensembles of Fe-Em interactions.

Charge of fragments Z	$\langle p_\perp \rangle$ in GeV/c		
	Fe-H	Fe-CNO	Fe-AgBr
2	0.31 ± 0.02	0.35 ± 0.01	0.39 ± 0.01
3 - 4	0.42 ± 0.06	0.47 ± 0.04	0.44 ± 0.03
5 - 8	0.43 ± 0.10	0.51 ± 0.05	0.57 ± 0.04
≥ 9*)	0.49	0.52	0.56

*) A crude estimate - see Table 4.

Table 6.   Coefficients of azimuthal asymmetry in different ensembles of Fe-Em collisions.

Ensemble of events	A	$\langle \alpha \rangle$
Fe-H	-0.07 ± 0.06	0.00 ± 0.11
Fe-CNO	-0.10 ± 0.03	0.24 ± 0.07
Fe-AgBr	-0.15 ± 0.03	0.32 ± 0.06
Fe-Em	-0.12 ± 0.02	0.25 ± 0.04
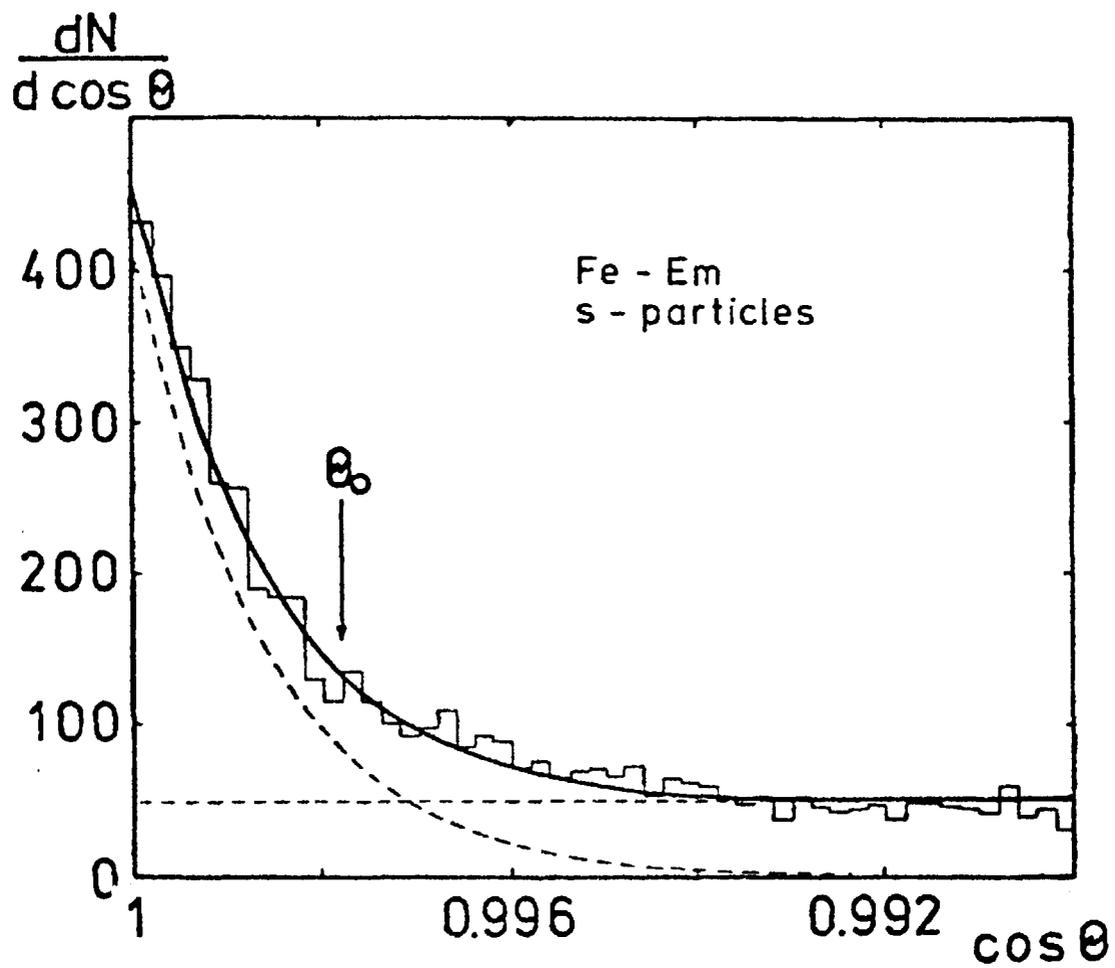
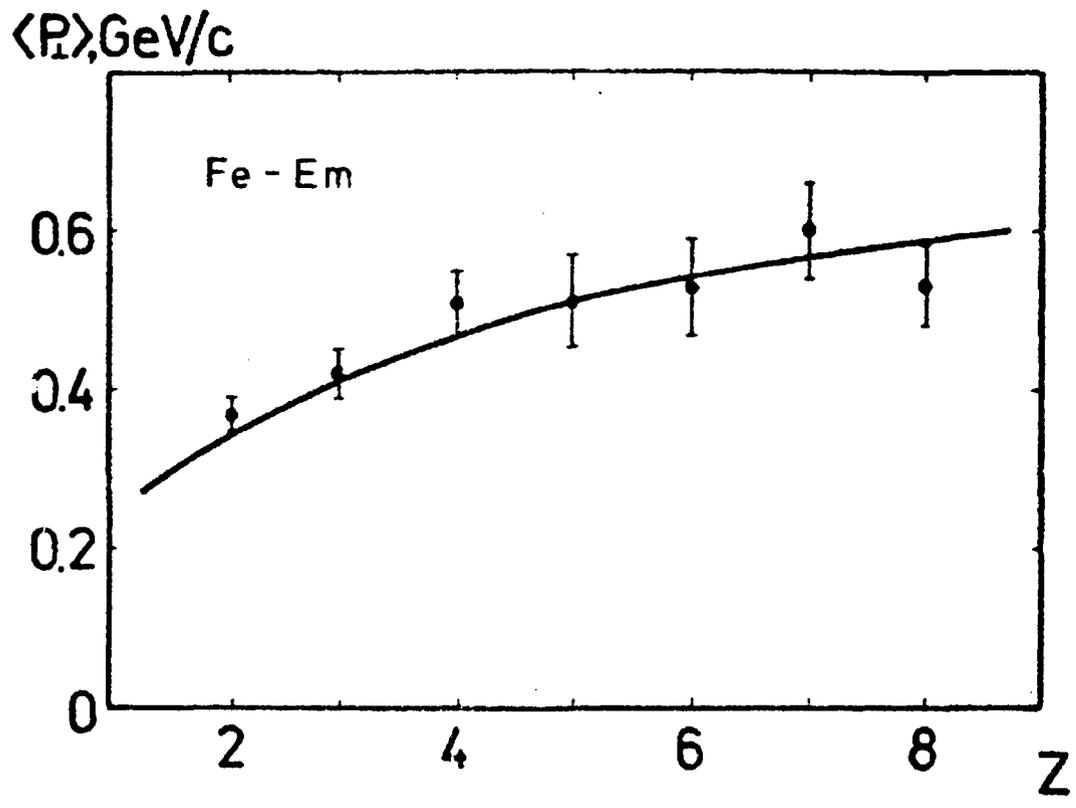Figure 1
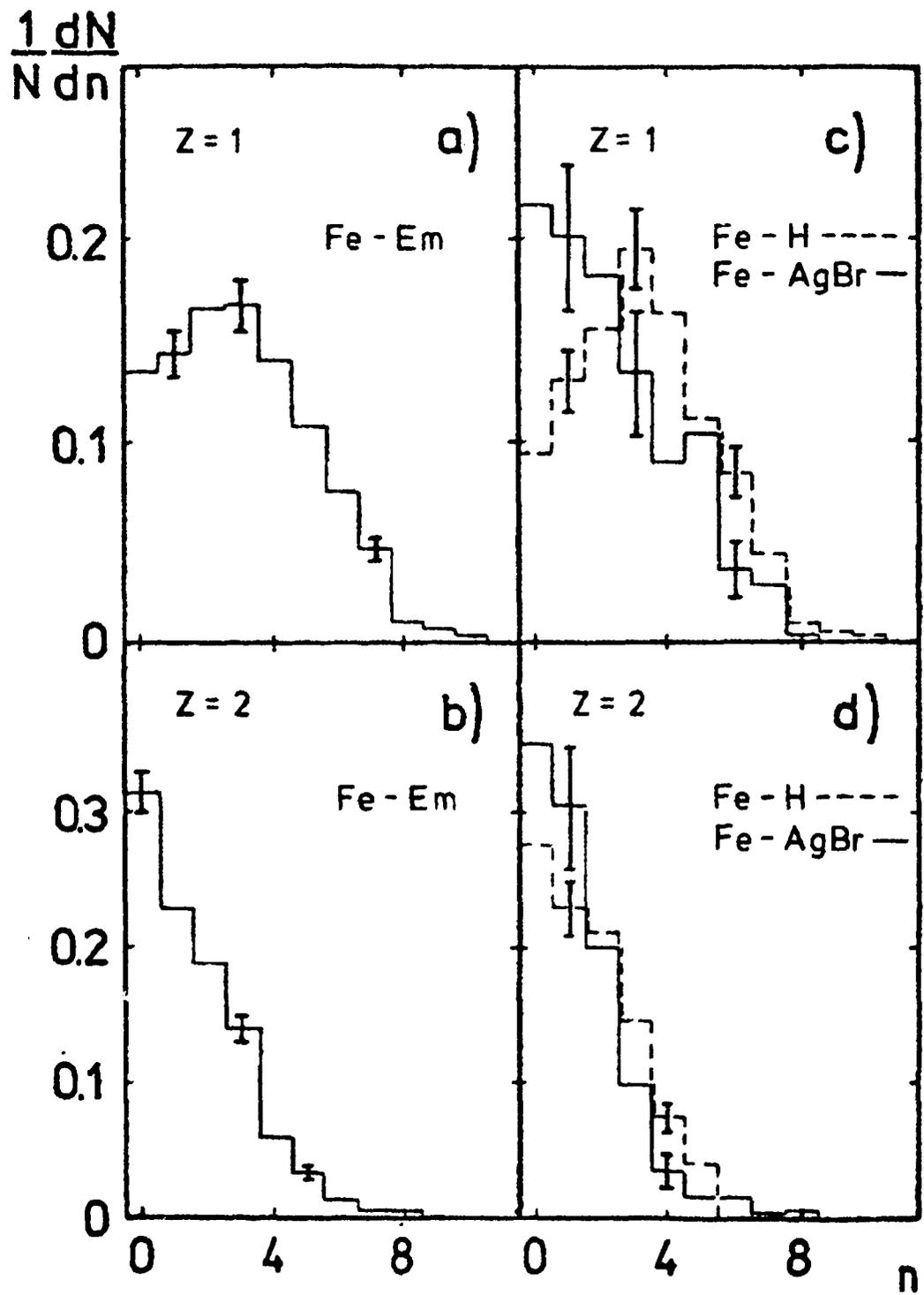
Figure 2
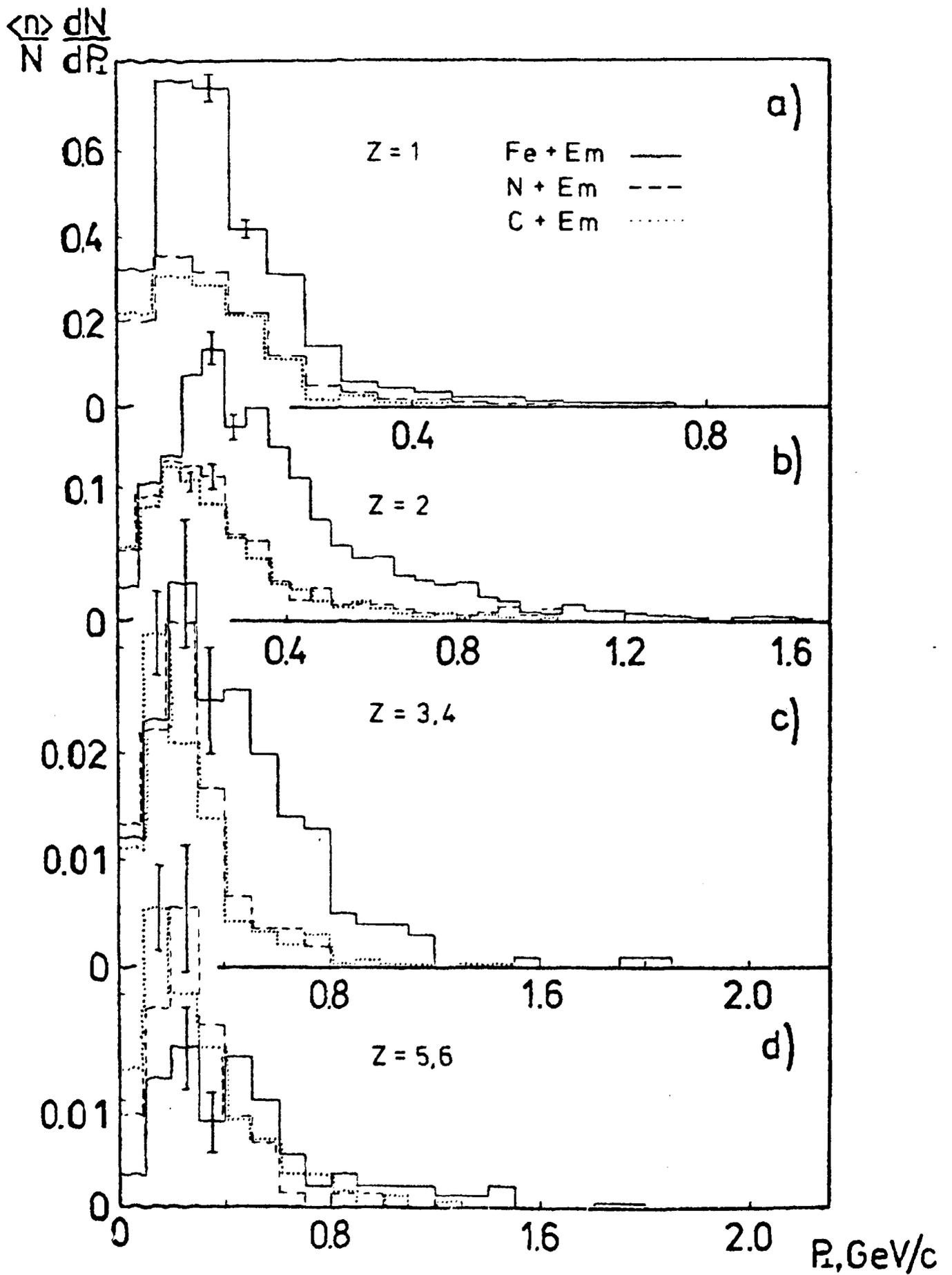
Figure 3
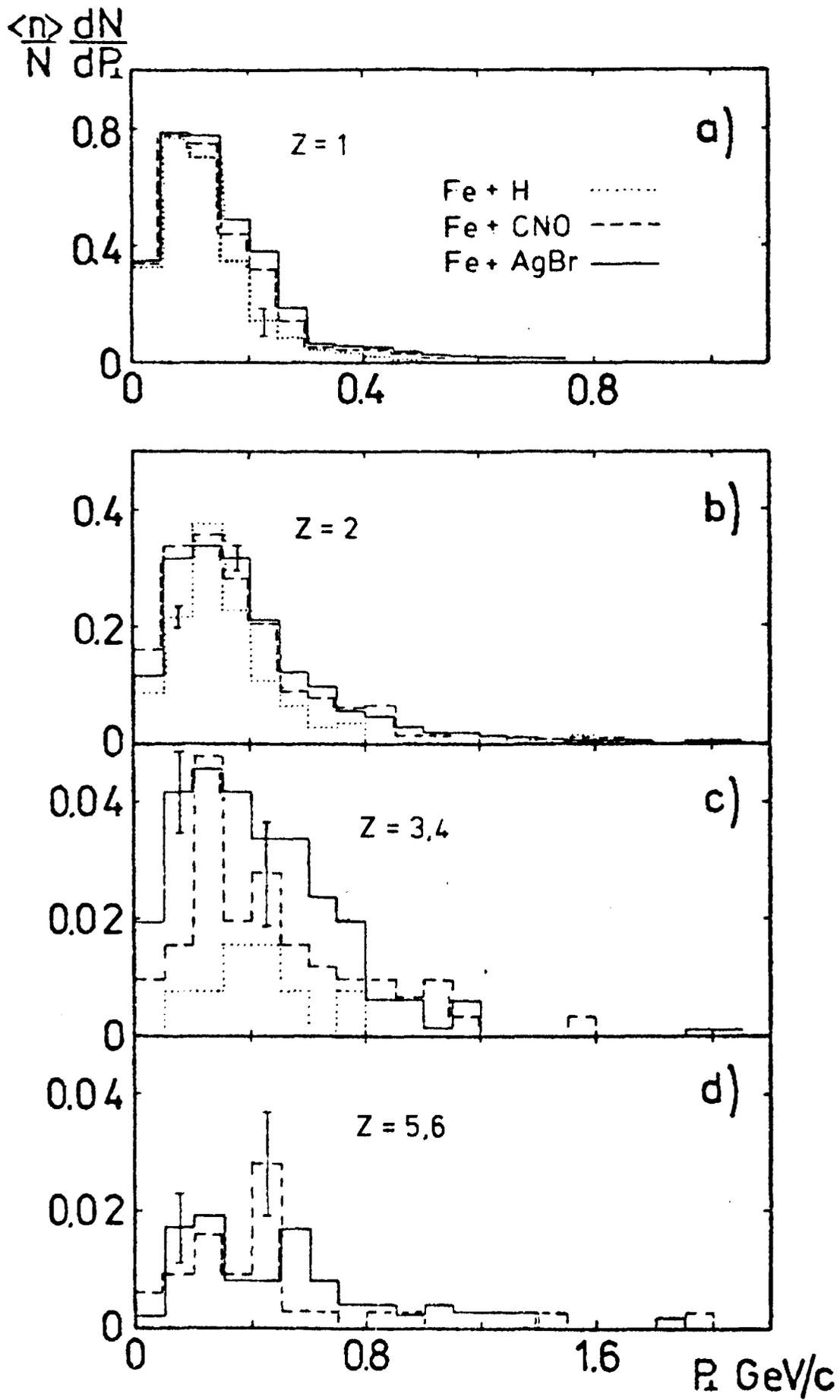
Figure 4
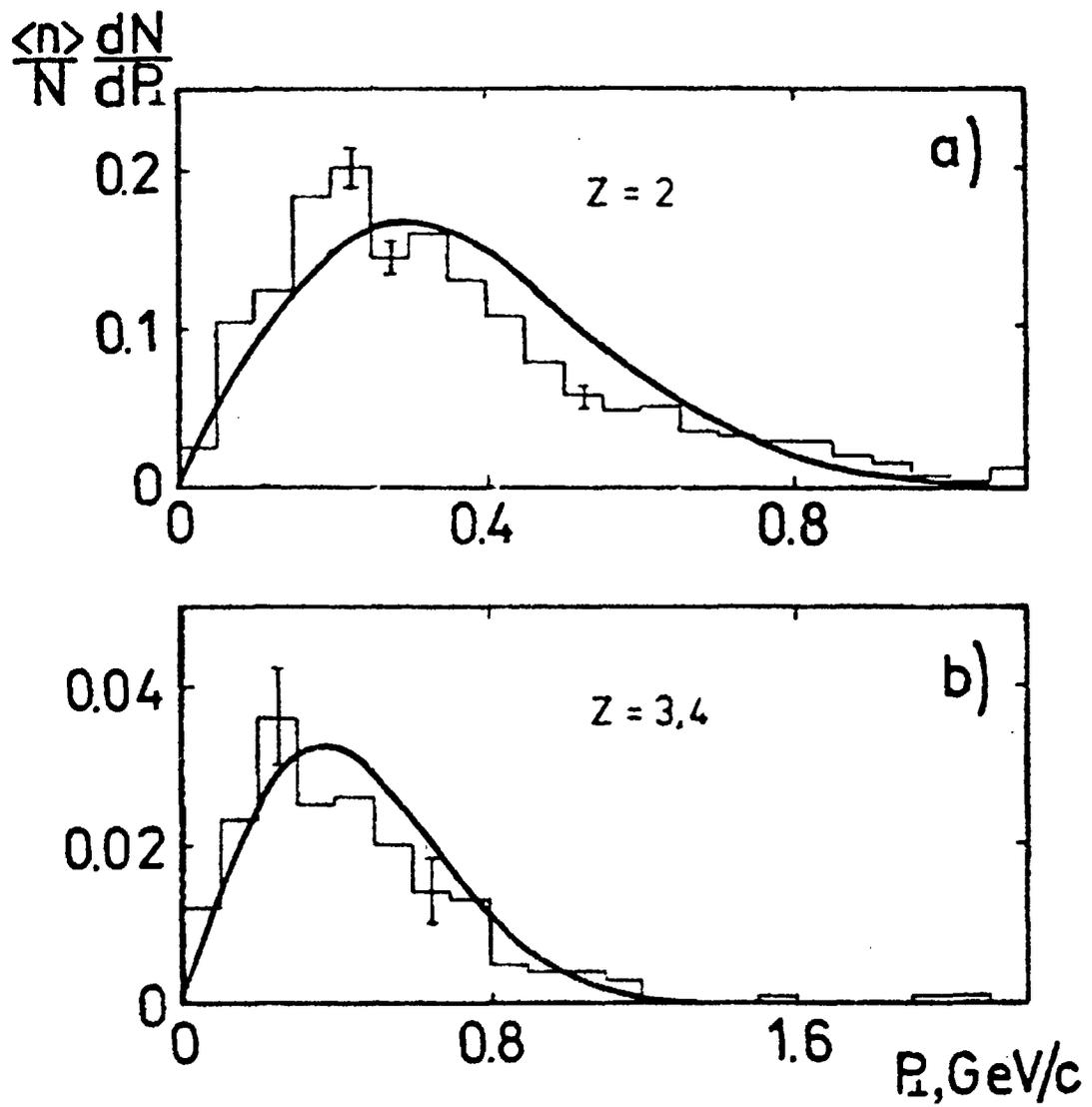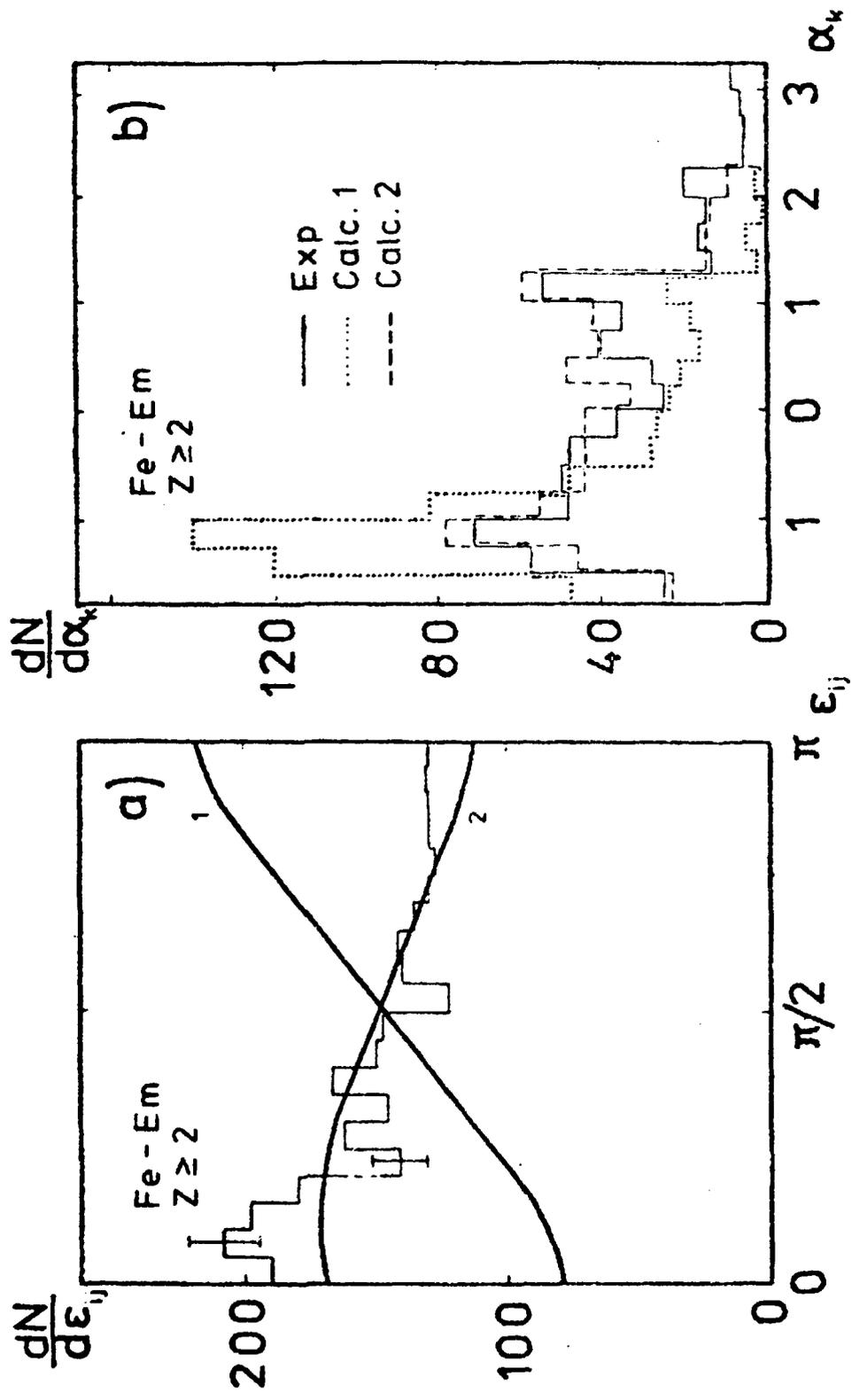
Figure 5

Figure 6

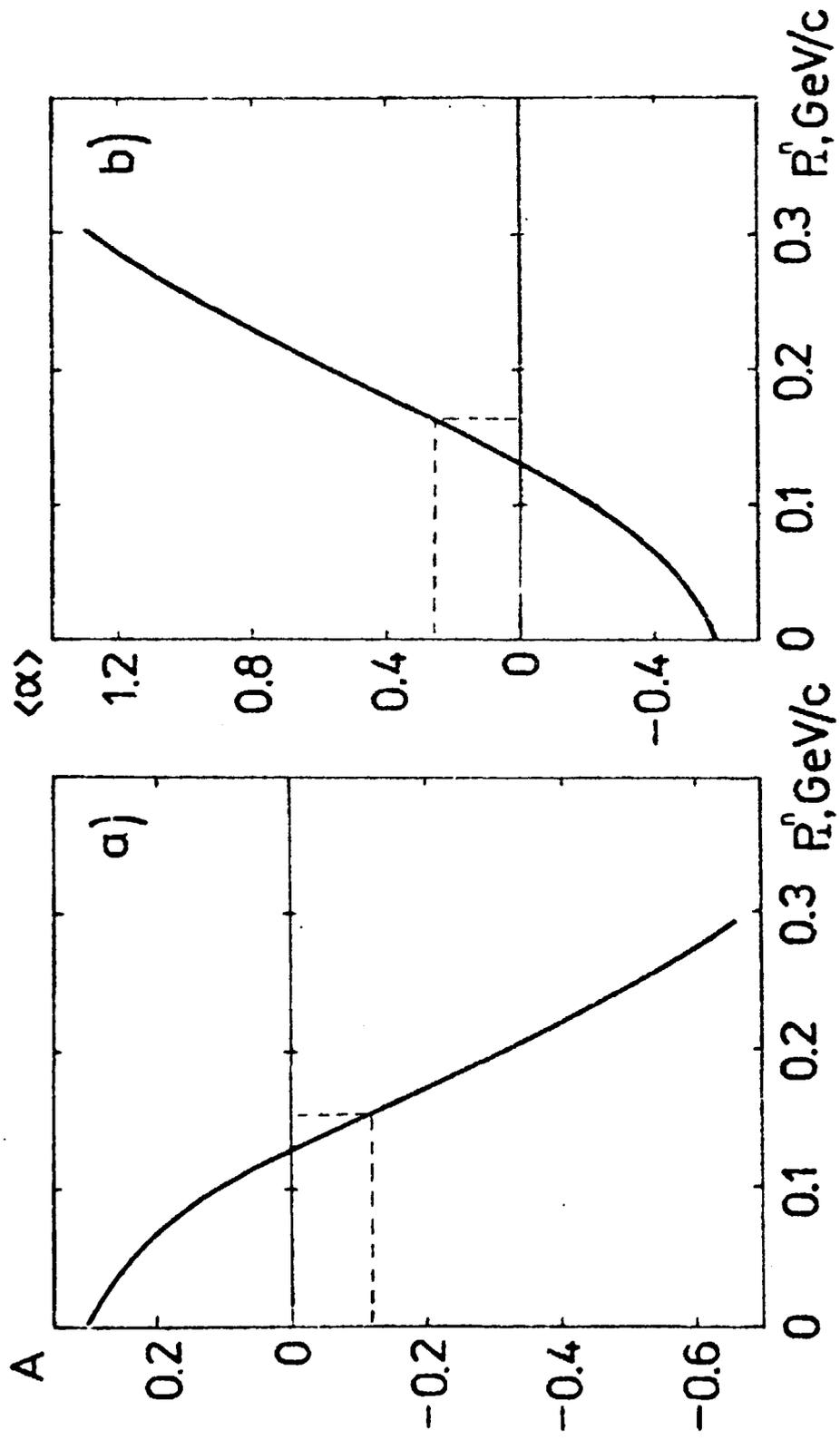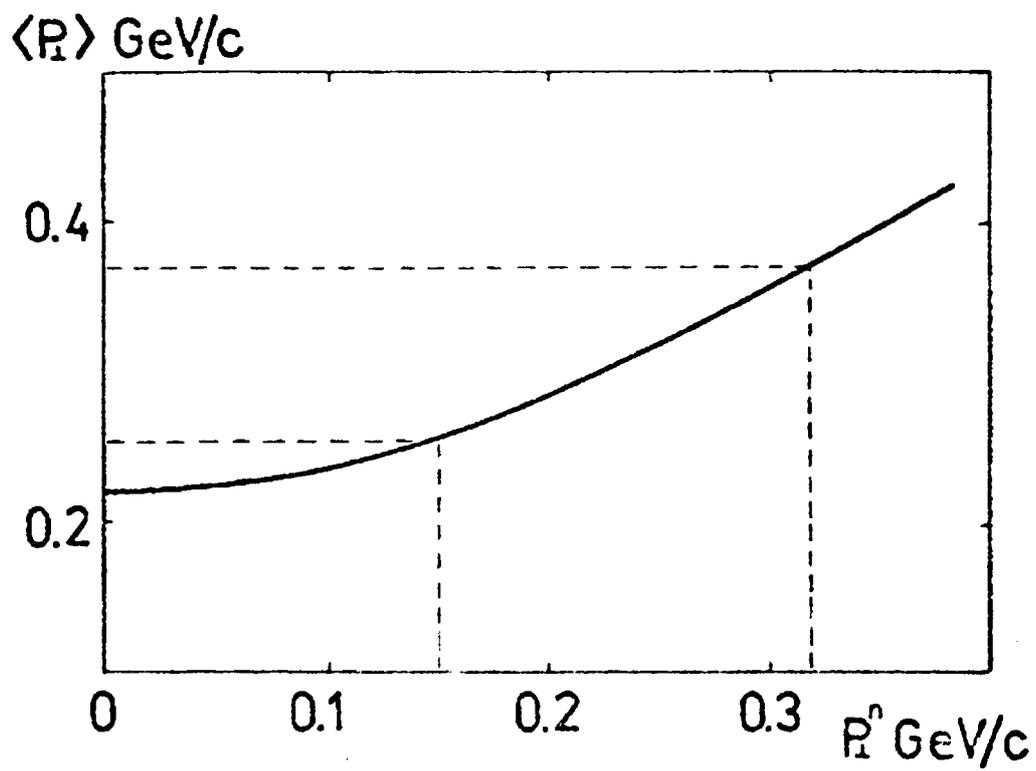Figure 7

Figure 8

Figure 9

Författare
    G.M. Chernov
    K.G. Gulamov
    U.G. Gulyamov
    V.Sh. Navotny
    N.V. Petrov
    L.N. Svechnikova
    B. Jakobsson
    A. Oskarsson
    I. Otterlund

Dokumenttitel och undertitel

FRAGMENTATION OF RELATIVISTIC ^{56}Fe NUCLEI IN EMULSION

Referat (sammandrag)

Experimental data on general characteristics of projectile fragments in inelastic interactions of relativistic ^{56}Fe nuclei in emulsion (multiplicities, transverse momentum distributions, azimuthal correlations) are presented and discussed.

A strong dependence on the mass number of the projectile nucleus is observed for the transverse momenta of the emitted projectile fragments. These fragments exhibit an azimuthal asymmetry caused by the transverse motion of the fragmenting residue. It is shown that this motion can be responsible only for a small part of the increase of the average transverse momentum of the fragments with increasing mass of the projectile.

Referat skrivet av
    The authors

Förslag till ytterligare nyckelord

Klassifikationssystem och -klass(er)

Indextermer (ange källa)

DOKUMENTDATABLAD enligt SIS 62 10 12

Blankett LU 11:25 1976--07